Dalton
www.rsc.org/dalton

Experimental and theoretical study of intramolecular exchange in $Ir_2Rh_2(CO)_{12}$ and $Ir_4(CO)_{11}(\mu\text{-}SO_2)$†

Zoltán Béni, Leonardo Guidoni, Gábor Laurenczy, Ursula Roethlisberger and Raymond Roulet*
Institute of Chemical Sciences and Engineering, Swiss Federal Institute of Technology, Lausanne, BCH, CH-1015, Lausanne, Switzerland. E-mail: raymond.roulet@epfl.ch

Received 30th September 2004, Accepted 29th October 2004
First published as an Advance Article on the web 30th November 2004

As observed by variable-temperature and -pressure ^{13}C NMR, intramolecular carbonyl scrambling in $Ir_2Rh_2(CO)_{12}$ and $Ir_4(CO)_{11}(\mu\text{-}SO_2)$ proceeds *via* a 'change of basal face' mechanism. In both cases the site exchange process has a positive activation volume suggesting that the transition states contain longer M–M distances compared to ground states of C_s symmetry. Transition state structures have been located by density functional calculations including relativistic effects. These structures contain a new symmetry plane which interchanges the indistinguishable starting and final geometries. Both transition state structures contain one significantly elongated M–M distance, bearing the bridging ligand unaffected by the site exchange. Differences in molecular volumes of ground and transition state geometries as calculated from Connolly surfaces and electron densities confirm the volume expansion in both cases. The sign of the activation volume is therefore a good criterion for distinguishing between the two main site exchange processes occurring in tetrahedral d^9 carbonyl clusters, *i.e.* the 'change of basal face' process and the 'merry-go-round' process, as the latter presents a negative activation volume.

Introduction

The bulk of the studies on the fluxional behaviour of cluster compounds have dealt with the migration of CO over tri- and tetrametallic carbonyl clusters[1–6] and have led to two theories of carbonyl scrambling.[7–9] A first mechanism of site exchange – the so called 'merry-go-round' – was proposed by Cotton in 1966,[7] and was supposed to take place *via* a transition state with all CO's in terminal positions. This type of site exchange was shown to take place in numerous tetrahedral clusters such as $Rh_4(CO)_{12}$ or $IrRh_3(CO)_{12}$. An NMR study of these two compounds showed that the activation volume of carbonyl scrambling has a negative value, which was confirmed by DFT calculations.[10] Statistical analysis of X-ray data[11,12] indicated as well that unbridged metal–metal distances (as postulated for the transition state) are shorter than bridged ones (as found in ground states).

A second mechanism of site exchange in the specific M_4 clusters is the so called 'change of basal face' which has been shown to take place in $Ir_4(CO)_{10}(\eta^2\text{-diarsine})$,[13] $Ir_2Rh_2(CO)_{12}$ (**1**) and $Ir_4(CO)_{11}(\mu\text{-}SO_2)$ (**2**).[14,15] In contrast with the 'merry-go-round' process bridge opening and closing do occur, but one bridging ligand of the ground state remains unaffected. The transition state of this fluxional process is unknown up to now. The possibility of differentiating this process from the 'merry-go-round' by the sign of its activation volume is still an open question. The aims of the present study are to propose a transition state structure for this carbonyl scrambling process and to answer the latter question.

Numerous studies have demonstrated the importance of including pressure as a kinetic parameter in the elucidation of inorganic reaction mechanisms.[16–18] The clusters $M_4(CO)_{12}$ are suitable for variable-pressure studies, as there is no charge creation or annihilation on forming the transition state. The electrostriction can therefore be neglected, and the activation volume, $\Delta V^{\#}$ can be deduced from variable-pressure NMR spectra using the equation $\ln k = \ln k_0 - (\Delta V^{\#} P/RT)$, where k_0 is the rate constant of the site exchange process at 0.1 MPa. This method has been used here to determine the activation volume of CO scrambling in **1** and **2**. Since these compounds have only one ground state structure in solution (no isomers) the value of $\Delta V^{\#}$ cannot be compared with reaction volumes. Therefore the experimental study had to be complemented by a DFT calculation in order to characterize transition states.

Results and discussion

Variable-pressure ^{13}C NMR study

The ground-state geometries of $Ir_2Rh_2(CO)_{12}$ (**1**) and $Ir_4(CO)_{11}(\mu\text{-}SO_2)$ (**2**) in solution have C_s symmetry with three ligands (3 CO's in **1** or 2 CO's and SO_2 in **2**) edge-bridging one $IrRh_2$ or one Ir_3 face, respectively.[14,15] Both clusters are fluxional above 230 K (**1**) and 210 K (**2**) with the dynamic connectivity b ↔ d ↔ g, f ↔ h, and e ↔ c (Fig. 1). Carbonyl a of **1** or the SO_2 ligand of **2** remain unaffected. This excludes site exchange by a merry-go-round of six CO's as proposed for $Rh_4(CO)_{12}$. Since restricted axial–basal site exchanges are observed, the fluxional processes may be called a 'change of basal face' *e.g.* M2–M4–Ir1 to M2–M4–Ir3. Eyring regression of $\ln(k/T)$ *vs.* $1/T$ gave free

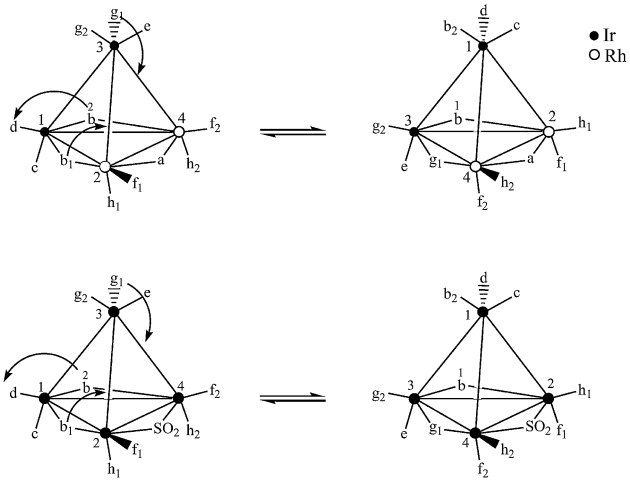

Fig. 1 Fluxional behaviour of clusters **1** and **2**.

† Electronic supplementary information (ESI) available: Distances (Å) in ground and transition state geometries of $Ir_2Rh_2(CO)_{12}$ (**1**) and $Ir_4(CO)_{11}(\mu\text{-}SO_2)$ (**2**) from geometry optimizations using ADF and Gaussian 03. Cartesian coordinates for calculated structures. See http://www.rsc.org/suppdata/dt/b4/b415147j/

DOI: 10.1039/b415147j

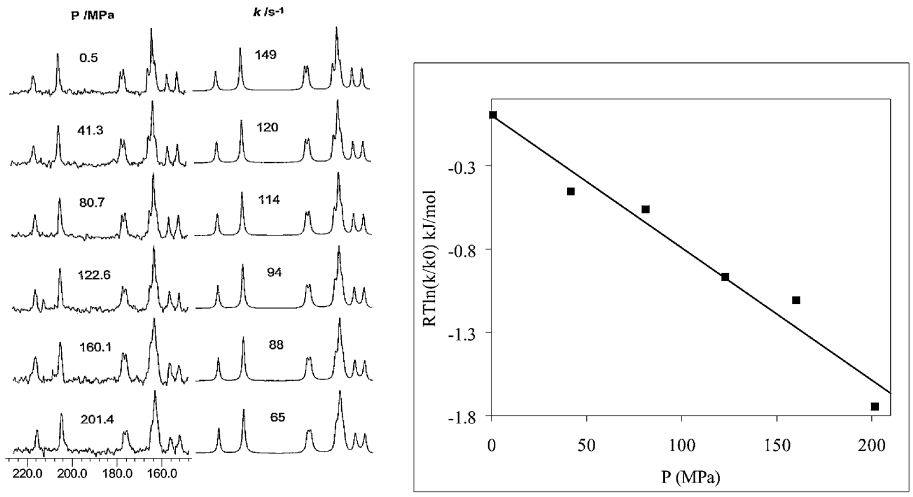

Fig. 2 VP ^{13}C NMR spectra of $Ir_2Rh_2(CO)_{12}$ at 254 K and its rate dependence on pressure.

enthalpies of activation of 51.2 ± 0.4 (**1**) and 47.2 ± 1.0 kJ mol^{-1} (**2**) at 298 K for the 'change of basal face' process.[14,15]

Using the same exchange matrices as those used to simulate the variable-temperature ^{13}C NMR spectra, a variable-pressure ^{13}C NMR study (example shown in Fig. 2, left) was undertaken in order to get experimental values for the activation volume of the site exchange process. Chosen temperatures were 254 K for **1** (Fig. 2, where k is the rate constant of CO scrambling) and 240 K for **2**. The values of k are given in the Experimental section.

Plotting $RT\ln(k/k_0)$ *vs.* P (Fig. 2, right) gave the following values of activation volume: $+7.9 \pm 0.8$ cm^3 mol^{-1} for **1** and $+15.1 \pm 0.6$ cm^3 mol^{-1} for **2** in CD_2Cl_2. In contrast with the negative values of $\Delta V^{\#}$ obtained for the merry-go-round process,[10,19] it appears that positive values of $\Delta V^{\#}$ are associated with the 'change of basal face'.

DFT study

To test the behaviour of different exchange functionals and basis sets in describing our systems, the ground state geometry of **2** was first optimized since its crystal structure is known,[14] while that of **1** was disordered. Calculations employed C_s symmetry and different density functionals, *i.e.* pure LDA with TZP basis set, GGA BP and TZP, GGA BLYP and TZP and GGA BLYP with TZ2P (see Experimental section for abbreviations). Concerning metal–metal and metal–sulfur bond lengths, LDA gave better agreement with experiment (the symmetrized crystal structure) than GGAs, while metal–carbon distances showed the opposite trend. Different GGA functionals (BP and BLYP) gave errors of similar magnitudes. Metal–metal distances were overestimated by 0.06 to 0.11 Å (2.08 to 4.12% relative errors) in the latter case. In all cases the most overestimated distances were: the Ir2–Ir4 (see Fig. 1 for numbering) bearing the bridging SO_2 ligand, Ir–S and S–O bond lengths. Increasing the basis set from TZP to TZ2P slightly improved the results (average deviations of metal–metal distances were 2.19% compared to 2.65%), but increased the computation time. On the basis of these findings and of the above referred study on similar systems[10] showing that LDA is sometimes better in terms of geometry but GGAs performs better for energetic, GGA with BLYP functional and TZP standard ADF basis sets were used in further calculations.

As shown in Fig. 1 the proposed mechanism deduced from 1D-VT and 2D ^{13}C NMR spectra of **1** and **2** (Fig. 2) include face switching of the M1M2M4 (M1 = Ir, M2,4 = Rh (**1**) or Ir (**2**)) to the M3M4M2 face. Carbonyl a (**1**) or SO_2 (**2**) is unaffected during the process, while g1 changes from terminal to bridging, b2 from bridging to terminal and b1 switches the bridging–edge from M1–M2 to M2–M3 (but not necessarily *via* face bridging as Shapley suggested[13]).

A synchronous linear transit (LT) search using 10 steps was undertaken to get a first estimate of the transition-state structures. A combination of three dihedral angles *i.e.* b1–, g1–M1M2M4 and b2–M1M3M4 were chosen as reaction coordinate and their synchronous change was able to describe the fluxional process of both clusters. Surprisingly, potential energy profiles of these LT calculations presented two almost isoenergetic maxima with a minimum in between (the largest energy differences were 6.5 and 3.7 kJ mol^{-1} for **1** and **2**, respectively). In the latter case refinement of the LT calculation with tighter convergence criteria resulted in even smaller (2.1 kJ mol^{-1}) energy difference. These findings indicate that the potential energy surfaces are rather flat near the transition states.

In terms of geometries, significant changes were found in the evolution of the M2–M4 (the metal–metal bond bridged by carbonyl a in **1** or by SO_2 in **2**) and M–C(a) (**1**) or M–S (**2**) distances. Significant elongation of the M2–M4 bond was observed till LT point 5 (from 2.80 to 3.04 Å in cluster **1**, from 2.88 to 3.41 Å in **2**). During this period carbonyl b became terminal on M2 with distances shortening from 2.15 to 1.95 Å in **1** and from 2.09 to 1.90 Å in **2**. Stabilization of M4 occurred *via* shortened M4–Ca (**1**) or M4–S (**2**) distances (from 2.12 to 2.02 Å and 2.453 to 2.32 Å, respectively). Simultaneously, carbonyl a or the SO_2 ligand flipped from the plane defined by the M2, M4 and M1 metal centres by 34.1 and 37.1° in **1** and **2**, respectively. The changes in M1–Cb and M3–Cb distances were not in agreement with the hypothetical face–bridged mechanism initially proposed by Shapley *et al*. for the site exchange in $Ir_4(CO)_{10}(\eta^2$-diarsine).[13] Analysis of the geometries at the LT points revealed that in the middle of the LT path both clusters adopt a geometry which has a new symmetry plane passing through Ca (or S in **2**) M2, M4 and Cb2. On the basis of group theory consideration it has been shown[20,21] that the transition states of chemical transformations can only have symmetry elements which are common to both reactants and products. In a fluxional process where starting and final geometries are indistinguishable, a transition state structure may have extra symmetry elements, but a new symmetry element has to interchange the starting and final states. In the present case the new symmetry plane obeys this rule for both clusters. It does not affect carbonyl a in **1** (or S in **2**) and interchanges M1↔M3, Cf1,2↔Ch1,2, Cb2↔Cg1, Cd↔Cg2 and Cc↔Ce as seen in Fig. 3. On the basis of these findings these geometries seemed to be close to the transition state structures. Geometry optimizations were then undertaken using the new symmetry plane (geometries are shown in Fig. 3).

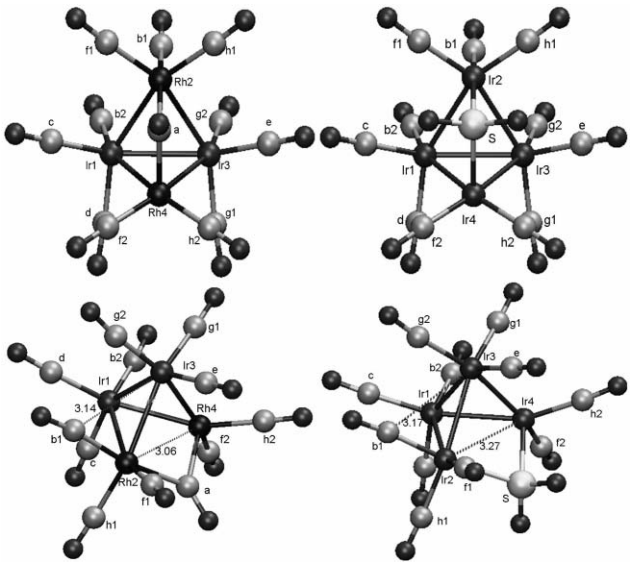

Fig. 3 Transition state geometries of **1** (left) and **2** (right) with C_s symmetry.

Due to C_s symmetry these geometries show equal distances for the M1–Cb and M2–Cb bonds (3.142 and 3.176 Å in **1** and **2**, respectively). This is in accordance with the fact that the transition states must be equidistant from, and have equal possibility to relax to, the starting and final points, since these are indistinguishable. The elongation of M2–M4 bond lengths compared to the ground state distances (see ESI†) is preserved and is larger for cluster **2** (0.392 compared to 0.261 Å). This is matching the experimentally observed activation volume differences (Table 1) assuming that volume change is dominated by varying size of the metal tetrahedron (this was shown to be true in the case of $Rh_4(CO)_{12}$ and $IrRh_3(CO)_{12}$[10]). Other metal–metal distances vary as well, but changes are smaller and similar for both clusters. The distances involving M4 are shortened while those involving M2 are elongated (due to increasing coordination number). Similarly the M2–Ca (or M2–S) distances are elongated while the corresponding bond lengths involving M4 are shortened.

Similar geometrical changes are observed in the corresponding ground- and transition-state structures of **1** and **2** optimized with the Gaussian software package (see ESI†). Due to the different basis set, all M–M, M–C, C–O distances are elongated by ~0.04 Å and by ~0.15 Å for M–S distances optimized in Gaussian 03 compared to those optimized in ADF.

A transition state corresponds to a first order stationary point on a potential energy surface that has a single negative Hessian eigenvalue corresponding to an imaginary frequency. The motion associated with this imaginary frequency is the motion which interconverts reactant and product close to the transition state. Therefore the calculation of the frequencies of a given structure can verify whether it is a transition structure or not. In the two DFT program packages these calculations are implemented differently, ADF calculates the frequencies numerically, while Gaussian does it analytically.

An ADF calculation was undertaken for cluster **2** and gave three imaginary frequencies associated with the geometry shown in Fig. 3 at 79, 71 and 23 cm^{-1}. Increasing the size of the integration grid still gave three imaginary frequencies at 79, 55 and 38 cm^{-1}. The fact that only the largest frequency, which is associated with the expected motion towards the final geometry, was not shifted indicated that the precision was still too low to correctly calculate these values. Unfortunately the numerical precision could not be further increased within an acceptable calculation time. Due to this drawback we repeated the calculation for **2** and achieved the calculation on cluster **1** using the Gaussian software package using analytical gradients. In the case of cluster **1** the calculation gave a single imaginary frequency at 31 cm^{-1} justifying that the suggested geometry was the transition state. In the case of cluster **2** two imaginary frequencies were found at 128.7 and 96.0 cm^{-1}. The rather low imaginary frequencies, together with their strong dependence on the used algorithm, suggest again that the region close to the transition state has a rather flat energy landscape. Based on this argument and the similarity of the two model systems, the structure presented in Fig. 3 having the new C_s symmetry is probably representative of the proper transition structure in the case of cluster **2** as well. For calculating molecular volumes this structure was used since more precise location of the proper saddle point of **2** could not be undertaken with an acceptable computational cost.

In terms of energies, ADF predicted barriers of 61.0 and 63.0 kJ mol^{-1} for cluster **1** and **2**, respectively, while Gaussian gives values 60.0 and 71.4 kJ mol^{-1}. These values are somewhat overestimated compared to the experimentally determined 51.2 ± 0.4 (**1**) and 47.2 ± 1 kJ mol^{-1} (**2**) free enthalpies of activation, probably because the calculation refers to molecules in the gas phase. The predicted barriers of the fluxional process of **1** were similar in both DFT packages, but Gaussian overestimated somewhat more the barrier in the case of **2**. Both packages confirmed that the face–bridged structures of **1** and **2** are the most stable ones. Additionally, ADF showed that the rearrangements of the two clusters need similar energies and that the type of exchange process is the same.

Molecular volumes were calculated for the optimized ground and transition state geometries with two methods. By using the Cerius[2] 3.0 software package[22] volumes were calculated based on Connolly surfaces,[23] while by Gaussian 03 molecular volumes were computed by integrating the volume occupied by electronic density that overcomes a certain threshold (typically 10^{-4} au).

Table 1 summarizes the results obtained by Cerius[2] using different probe radii for the structures optimized in ADF and in Gaussian software packages. The volume of an independent cluster molecule was calculated to be about 420 $Å^3$ which is in good agreement with the volume of a sphere having a radius of 4.6 Å (1.15 + 1.9 + 1.55 Å, respectively for C–O and C–M distances and for the distance between a metal atom and the centre of mass of a regular tetrahedron with apexes at 2.85 Å). The volumes of **2** in its ground state and in the transition state are somewhat larger than the corresponding volumes of **1**, which is in good agreement with larger metal–metal distances in **2** and with increasing ligand size on going from CO to SO_2. The activation volumes were calculated by subtracting the corresponding volumes of ground states and transition states obtained from geometry optimizations using ADF and Gaussian software packages. The calculated activation volume of **1** (+2.5 cm^3 mol^{-1} for a probe radius of 2.0 Å in the case of ADF optimized structures and +4.9 cm^3 mol^{-1} for geometries optimized in Gaussian) and **2** (+4.5 and +8.6 cm^3 mol^{-1}, respectively) are

Table 1 Calculated $\Delta V^{\#}$ (cm^3 mol^{-1}) for structures optimized using ADF and Gaussian 03

Probe radius/Å	$\Delta V^{\#}$ (**1** opt. in ADF)	$\Delta V^{\#}$ (**1** opt in Gaussian 03)	$\Delta V^{\#}$ (**2** opt. in ADF)	$\Delta V^{\#}$ (**2** opt. in Gaussian 03)
1.8	2.0	4.4	6.2	5.6
2.0	2.5	4.9	4.5	8.6
2.2	2.9	4.6	4.6	9.4
2.4	1.8	3.4	9.0	7.5

smaller compared to the experimentally observed values of $+7.9 \pm 0.8$ (**1**) and $+15.1 \pm 0.6$ cm^3 mol^{-1} (**2**). Nevertheless the predicted smaller value for **1** and the positive sign of both activation volumes are in agreement with experiment.

Calculation of molecular volumes by integrating the volume occupied by electronic density gave values of activation volume of $+0.8 \pm 0.3$ cm^3 mol^{-1} for **1** and of $+3.1 \pm 0.4$ cm^3 mol^{-1} for **2** which are smaller than those calculated with Connolly surfaces.

In conclusion both methods predicted volume expansion during the fluxional processes in **1** and **2**, the latter being larger. This is in accordance with experimental results, although the numerical values are smaller than the experimental values.

Site exchange of a ligand other than CO

It has been shown that site exchange in **1** and **2** requires edge-switching of a CO ligand while the non-exchanging, bridging ligand rocks about its own edge. It would be interesting to see if edge-switching of a ligand different from CO would also lead to a positive value of activation volume. A candidate for such a study is the phosphido–cluster $Rh_4(CO)_6(\mu\text{-}PPh_2)_4$, since a ^{103}Rh, ^{31}P and ^{13}C NMR study in CD_2Cl_2 has indicated that the strongly bonded, bridging, anionic ligand PPh_2^- takes part in the site exchange of carbonyl ligands and is actually mobile about the metallic surface of this cluster compound.[24,25] The ground state structure determined by Lau *et al.*[26] is shown in Fig. 4 (left). The observed exchanges are P1↔P3, C2↔C5 and C3↔C6. It was conclusively shown by a variable-temperature ^{13}C and ^{31}P NMR study that the process leading to P1↔P3 exchange is P4 switching to the Rh1–Rh3 edge, terminal C5 bridging the Rh1–Rh4 edge and μ-C2 becoming terminal on Rh1.[24]

We therefore recorded the variable-pressure ^{31}P NMR spectra of $Rh_4(CO)_6(\mu\text{-}PPh_2)_4$ at 253 K in CD_2Cl_2 and simulated these spectra using a simple two site exchange matrix (P1↔P3). The results are shown in Fig. 4 (right) with the experimental values of the rate constant k in the experimental part. Plotting $RT\ln(k/k_0)$ *vs.* P gave a value of $+ 9.9 \pm 0.6$ cm^3 mol^{-1} for the activation volume. Therefore, edge-switching of PPh_2^- (μ-P_4 in Fig. 4) is also associated with a positive activation volume.

Unfortunately, we do not know how general this result is as we could not find another cluster compound showing an edge-switch of a ligand different from CO and PPh_2^- and exchanging sites in the NMR kinetic window.

Conclusion

Earlier DFT calculations[10] have shown that the merry-go-round process is characterized by a volume contraction in the transition state. The present DFT calculations have shown that the 'change of basal face' process is accompanied by a volume expansion in the transition state (Table 2).

Therefore, one may propose that the experimentally determined sign of the activation volume is a good criterion to distinguish between the two main site exchange processes taking place in tetrahedral carbonyl clusters. It may intuitively be expected that the transition state of the 'change of basal face' would have a symmetry plane bisecting the angle between the initial bridged face and the final one. This was confirmed by our DFT calculation. Shapley *et al.* proposed that carbonyl exchange could take place *via* a face–bridged mechanism, as this coordination mode is also known for CO (or PPh_2^-). This was confirmed by our calculation.

Table 2 Activation volumes of carbonyl clusters

Type of site exchange	Cluster	Activation volume $\Delta V^{\#}$ (cm^3 mol^{-1})
Merry-go-round	$Rh_4(CO)_{12}$	-6.0 ± 1.0[19]
	$IrRh_3(CO)_{12}$	-7.7 ± 0.6[19]
	$Ir_4(CO)_9P(OPh)_3$	-8.3 ± 0.2[19]
Change of basal face	$Ir_2Rh_2(CO)_{12}$	$+7.9 \pm 0.8$
	$Ir_4(CO)_{11}(\mu\text{-}SO_2)$	$+15.1 \pm 0.6$
PPh_2^- exchange	$Rh_4(CO)_6(\mu\text{-}PPh_2)_4$	$+9.9 \pm 0.6$

Experimental

Samples enriched in ^{13}CO (~25%): $Ir_2Rh_2(CO)_{12}$, $Ir_4(CO)_{11}(\mu\text{-}SO_2)$ and $Rh_4(\mu\text{-}PPh_2)_4(CO)_6$ were synthesized according to literature methods.[7,14,15,24,26] The ^{13}C NMR spectra at variable pressure were recorded on Bruker AC 200 (50.323 MHz) for $Ir_2Rh_2(CO)_{12}$ (254 K) and $Ir_4(CO)_{11}(\mu\text{-}SO_2)$ (240 K). The measurements were made up to 2000 bar using a home-built high-pressure probe.[27] A built-in platinum resistor allowed temperature measurements with an accuracy of ±1 K. When a thermostated liquid was pumped through the bomb, the temperature was stabilized to ±0.2 K. ^{13}C and ^{31}P chemical shifts are referred to external TMS (measured with respect to the solvent CD_2Cl_2 signal at 53.2 ppm) and external 85% H_3PO_4, respectively. The exchange matrices used for spectral simulation are the same as those previously used[14,15] for simulation of the VT spectra. The kinetic data for **1** are given in Fig. 2, for **2**: values of k in s^{-1} at 240 K (P in MPa): 698 (1.3), 527 (50.8), 311 (98.0), 243 (149.8); for $Rh_4(CO)_6(\mu\text{-}PPh_2)_4$ at 253 K: 198 (4.8), 172 (18.8), 139 (46), 127 (89.8), 90 (153.3). 79 (189.1).

All computations were carried out using Amsterdam Density Functional (ADF)[28–30] and Gaussian 03[31] software packages. In ADF the Vosko–Wilk–Nusair (VWN)[32] parametrization of the electron gas for local density approximation (LDA) and exchange-correlation functionals from Becke and Perdew[33,34] (BP) and Becke–Lee–Yang–Parr[35–37] (BLYP) for the generalized gradient approximation (GGA) were used. Relativistic zero-order regular approximation (ZORA) was applied.[38,39] As basis set triple-zeta Slater-type orbitals with p polarization functions were used for all elements as implemented in the ADF basis set library (ZORA/TZP).[30] The frozen core approximation was used to treat electrons in lower shells (Rh, 1s–3d; Ir, 1s–4d; S, 1s–3p; C and O, 1s). Calculation within the Gaussian 03 software

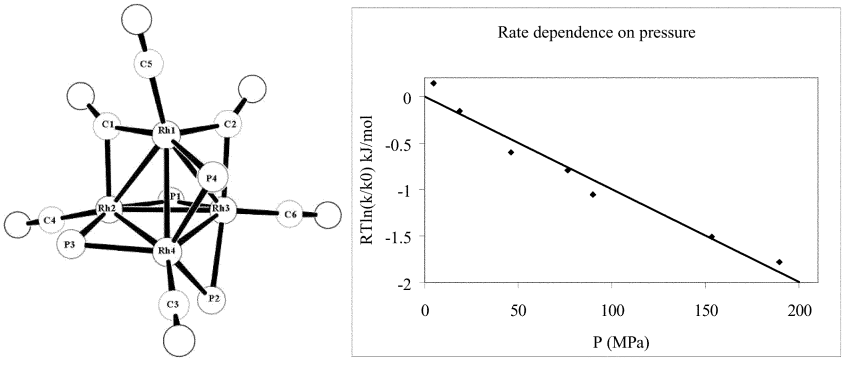

Fig. 4 Structure of $Rh_4(CO)_6(\mu\text{-}PPh_2)_4$ (left).[26] Rate constant of PPh_2^- exchange as function of pressure (right).

package, employed BLYP functional and Stuttgart/Dresden MWB[40] basis sets for all elements.

Molecular volumes were calculated from Connolly surfaces[23] and from electron densities. Connolly surface volumes were obtained by the Cerius^2 3.0[22] software package with probe radii ranging from 1.8 to 2.4 Å and with a dot density of 100 Å^{-2}. Electron density volumes were calculated using the 'Volume' keyword in Gaussian 03 with 10^{-3} e bohr^{-3} envelope and 10^4 points bohr^{-3}.

References

1 B. F. G. Johnson and A. Rodgers, in *The Chemistry of Metal Cluster Complexes*, ed. D. F. Schriver, H. D. Kaesz and R. D. Adams, VCH, 1990.
2 S. Aime, W. Dastru, R. Gobetto, J. Krause and L. Violano, *Inorg. Chim. Acta*, 1995, **235**, 757.
3 H. Adams, X. Chen and B. E. Mann, *J. Chem. Soc., Dalton Trans.*, 1996, 2159.
4 R. Roulet, in *The Synergy Between Dynamics and Reactivity at Clusters and Surfaces*, ed. L. J. Farrugia, NATO, ASI Series, Kluwer Academic Publications, Dordrecht, 1995, p. 159.
5 L. J. Farrugia, J. Orpen and A. Guy, *Met. Clusters Chem.*, 1999, **2**, 1001.
6 L. J. Farrugia, *J. Chem. Soc., Dalton Trans.*, 1997, 1783.
7 F. A. Cotton, *Inorg. Chem.*, 1966, **5**, 1083.
8 B. F. G. Johnson and R. E. Benfield, *J. Chem. Soc., Dalton Trans.*, 1978, 1554.
9 B. F. G. Johnson and Y. V. Roberts, *Inorg. Chim. Acta*, 1993, **205**, 175.
10 K. Besancon, G. Laurenczy, T. Lumini, R. Roulet, R. Bruyndonckx and C. Daul, *Inorg. Chem.*, 1998, **37**, 5634.
11 D. Braga, F. Grepioni, J. J. Byrne and M. J. Calhorda, *J. Chem. Soc., Dalton Trans.*, 1995, 3287.
12 D. Braga and F. Grepioni, *J. Organomet. Chem.*, 1987, **336**, C9.
13 J. R. Shapley, G. F. Stunz, M. R. Churchill and J. P. Hutchinson, *J. Am. Chem. Soc.*, 1979, **101**, 7425.
14 D. Braga, R. Ros and R. Roulet, *J. Organomet. Chem.*, 1985, **286**, C8.
15 G. Bondietti, G. Suardi, R. Ros, R. Roulet, F. Grepioni and D. Braga, *Helv. Chim. Acta*, 1993, **76**, 2913.
16 R. Van Eldik, T. Asano and W. le Noble, *Chem. Rev.*, 1989, **89**, 549.
17 A. E. Merbach, *Pure Appl. Chem.*, 1987, **59**, 161.
18 G. Laurenczy, A. E. Merbach, B. Moullet, R. Roulet, L. Hoferkamp and G. Süss-Fink, *Helv. Chim. Acta*, 1993, **76**, 2936.
19 K. Besancon, PhD thesis, University of Lausanne, Switzerland, 1996.
20 P. Pechukas, *J. Chem. Phys.*, 1976, **64**, 1516.
21 R. E. Stanton and W. J. McIver, *J. Am. Chem. Soc.*, 1975, **97**, 3632.
22 Cerius 2 3.0, MSI Cambridge, UK.
23 M. L. Connolly, *J. Am. Chem. Soc.*, 1985, **107**, 1118.
24 E. Gullo, S. Detti, G. Laurenczy and R. Roulet, *J. Chem. Soc., Dalton Trans.*, 2002, 4577.
25 R. J. Crowte and J. Evans, *J. Chem. Soc., Chem. Commun.*, 1984, 1332.
26 C. P. Lau, C. Y. Ren, L. Book and T. C. W. Mak, *J. Organomet. Chem.*, 1983, 249.
27 U. Frey, L. Helm and A. E. Merbach, *High Pressure Res.*, 1990, **2**, 237.
28 C. Fonseca Guerra, O. Visser, J. G. Snijders, G. te Velde and E. J. Baerends, in *Parallelization of the Amsterdam Density Functional Program*, Cagliari, 1995.
29 G. te Velde, F. M. Bickelhaupt, E. J. Baerends, S. J. A. van Gisbergen, C. Fonseca Guerra, J. G. Snijders and T. Ziegler, *J. Comput. Chem.*, 2001, **22**, 931.
30 *Amsterdam Density Functional, Theoretical Chemistry*, Vrije Universiteit, Amsterdam, 2003.
31 M. J. Frisch, G. W. Trucks, H. B. Schlegel, G. E. Scuseria, M. A. Robb, J. R. Cheeseman, J. A. Montgomery, J. T. Vreven, K. N. Kudin, J. C. Burant, J. M. Millam, S. S. Iyengar, J. Tomasi, V. Barone, B. Mennucci, M. Cossi, G. Scalmani, N. Rega, G. A. Petersson, H. Nakatsuji, M. Hada, M. Ehara, K. Toyota, R. Fukuda, J. Hasegawa, M. Ishida, T. Nakajima, Y. Honda, O. Kitao, H. Nakai, M. Klene, X. Li, J. E. Knox, H. P. Hratchian, J. B. Cross, C. Adamo, J. Jaramillo, R. Gomperts, R. E. Stratmann, O. Yazyev, A. J. Austin, R. Cammi, C. Pomelli, J. W. Ochterski, P. Y. Ayala, K. Morokuma, G. A. Voth, P. Salvador, J. J. Dannenberg, V. G. Zakrzewski, S. Dapprich, A. D. Daniels, M. C. Strain, O. Farkas, D. K. Malick, A. D. Rabuck, K. Raghavachari, J. B. Foresman, J. V. Ortiz, Q. Cui, A. G. Baboul, S. Clifford, J. Cioslowski, B. B. Stefanov, G. Liu, A. Liashenko, P. Piskorz, I. Komaromi, R. L. Martin, D. J. Fox, T. Keith, M. A. Al-Laham, C. Y. Peng, A. Nanayakkara, M. Challacombe, P. M. W. Gill, B. Johnson, W. Chen, M. W. Wong, C. Gonzalez, and J. A. Pople, *Gaussian*, Gaussian Inc., 2003.
32 S. H. Vosko, L. Wilk and M. Nusair, *Can. J. Phys.*, 1989, **58**, 1200.
33 A. D. Becke, *Phys. Rev. A*, 1988, **38**, 3098.
34 J. P. Perdew, *J. Phys. Rev. B*, 1986, **33**, 8822.
35 C. Lee, W. Yang and R. G. Parr, *Phys. Rev. B*, 1988, **37**, 785.
36 B. G. Johnson, P. M. W. Gill and J. A. Pople, *J. Chem. Phys.*, 1993, **98**, 5612.
37 T. V. Russo, R. L. Martin and P. J. Hay, *J. Chem. Phys.*, 1994, **101**, 7729.
38 E. van Lenthe, E. J. Baerends and J. G. Snijders, *J. Chem. Phys.*, 1993, **99**, 4597.
39 E. van Lenthe, *The ZORA equation*, Vrije Universiteit, Amsterdam, 1996.
40 M. Dolg, H. Stoll, H. Preuss and R. M. Pitzer, *J. Phys. Chem.*, 1993, **97**, 5852.